Journal Name

COMMUNICATION

Macroscopic crystalline deformation in an organic dye during reversible phase transition caused by alkyl disorder †

Received 00th January 20xx,
Accepted 00th January 20xx

DOI: 10.1039/x0xx00000x

www.rsc.org/

Takaya Minami, [a] Hiroyasu Sato [b] and Shinya Matsumoto*[a]

Single crystals of a bisazomethine dye with diethylamino terminal groups exhibited thermally induced dynamic behavior. DSC and microscopic measurements indicated that the crystal shape deformed reversibly owing to phase transition. The X-ray structural analysis revealed that the dynamic behavior was correlated with the disorder of the ethyl moieties.

Materials that exhibit dynamic behavior in response to external stimuli such as heat and light have attracted significant attention because of their potential applications in smart materials, such as artificial muscles, actuators, sensors, and biomimetic kinematic devices.[1-9] Rapidity, reversibility, and durability of the dynamic motion are required for practical use of these materials. Recently, studies regarding the macroscopic dynamic behavior of single crystals have been performed,[10-14] because of their efficient external energy transfer to mechanical motion and rapid motion owing to a dense and regularly ordered molecular environment. Studies on single crystals are also advantageous as they afford detailed structural data by X-ray analysis. Organic crystals, including metal-organic complexes, can control their molecular arrangement by a simple molecular modification.[15] In 1983, the phenomenon in which crystals jumped up in response to thermal stimulation was first reported by Etter and Siedle for (phenylazophenyl) palladium hexafluoroacetylacetonate.[16] The phenomenon was subsequently named the "thermosalient effect" by Gigg and collaborators in 1987. Afterwards, Naumov *et al.* eagerly studied this effect.[17-22] Their results indicated that this effect is characterized by a sharp phase transition accompanied by an anisotropic change of the unit cell, with a similar crystal structure with identical space groups before and after the transition, and a characteristic saw-tooth profile in the differential scanning calorimetry (DSC) curve at the transition. Recently, another interesting example of crystal deformation caused by an order-disorder phase transition was reported by Sato *et al.*.[23,24] They found that a crystalline cobalt (II) complex with an *n*-butyl group on its ligands exhibited thermally induced, abrupt, and reversible macroscopic shrinkage and expansion resulting in macroscopic dynamic behavior. This behavior was reported to originate from an order-disorder phase transition due to the rotation around the C-C bond of the butyl group, resulting in 6-7% change in its crystal size along the molecular packing direction. The authors also suggested that the introduction of an alkyl chain to the ligands would be a promising method to induce thermally responsive crystalline deformation. Herein, we report the crystal structure of an organic dye showing macroscopic deformation caused by the disorder of its terminal alkyl moieties. To the best of our knowledge, this is the first example of macroscopic crystalline deformation in metal-free organic crystals caused by the disorder of an alkyl moiety.

N,N'-bis[4-(*N,N*-diethylamino)benzylidene]diaminomaleonitrile (DE2)[25] (Sheme S1, ESI †) formed J-aggregates in thin deposited films and can be further applied to organic solar cells and field-effect transistors.[26-32] Its crystal structure analysis indicated that DE2 undergoes a structural phase transition at a low temperature (LT, 93 K).[33] The volume of the unit cell at LT is twice that of a room temperature (RT, 293 K) phase, and the number of molecules in the unit cell changes from $Z = 3$ ($Z' = 1.5$) to $Z = 6$ ($Z' = 3$). There were no significant differences in the geometries or molecular arrangements between the RT and LT phases. In the RT phase, the molecules are stacked along the [-1 1 1] direction in an -A-B-B-A-B-B- pattern (Fig. S1a, ESI †), where each A and B molecule is an independent molecular unit. The conformations of the ethyl moieties at the terminal diethylamino groups and dihedral angles of the aromatic rings differed between A and B in the RT phase. Unusual bond lengths associated with the terminal diethylamino groups were

[a] *Graduate School of Environmental and Information Sciences, Yokohama National University, 79-7 Tokiwadai, Hodogaya-ku, Yokohama 240-8501, Japan. E-mail: matsumoto-shinya-py@ynu.ac.jp*
[b] *Rigaku Corporation, 3-9-12 Matsubara-cho, Akishima, Tokyo 196-8666, Japan. E-mail: h-sato@rigaku.co.jp*

†Electronic Supplementary Information (ESI) available: Experimental details, crystallographic data, and the movies of crystalline deformation. CCDC 1811066–1811071, 1811081. For ESI and crystallographic data in CIF or other electronic format see DOI: 10.1039/x0xx00000x

observed for both molecules A and B.[34] The least squares planes of the conjugated system of DE2 for A and B were not parallel to each other, and instead were stacked with a tilt angle of 23.7° (Fig. S1b, ESI †). The centroids of the molecules were located at a distance of approximately one-third of the unit cell (Fig. S2, ESI †). Therefore, we expected that a further phase transition would occur with the change in the lattice volume and *Z* in the crystal of DE2. We then performed X-ray measurements on the DE2 crystals at high temperatures.

The prismatic single crystals of DE2 used for the experiments were obtained by a vapor-liquid diffusion method using a combination of chloroform and diethyl ether. DSC measurements revealed that the DE2 crystals exhibit an endothermic peak at 437 K, below the melting point of 551 K. Heating and cooling cycles were performed in the temperature range between 373 and 473 K with a heating rate of 20 K min^{-1} (Fig. 1). The DE2 crystals exhibited an endothermic peak upon heating and an exothermic peak upon cooling at approximately 436 and 420 K, respectively, with high reproducibility. Because of the relatively large thermal hysteresis of 15 K and their sharp peak shapes, this phase transition was considered to be a first-order phase transition.[23] Single crystal X-ray measurements of DE2 at 443 K indicated that the RT phase is transformed to the expected high-temperature (HT) phase whose unit cell volume is one-third of that of the RT phase (Table S1, ESI †). The number of the molecules in the unit cell is simultaneously decreased from three to one. During these experiments, the DE2 crystals exhibited reversible macroscopic deformation (Fig. 2 and movie S1-S6, ESI †). This macroscopic deformation was repeatable at least two times while preserving the crystallinity of DE2 (Fig. S3 ESI †), and at least five times from microscopic observation. The time for the motion was observed in the range from approximately 0.5-2 s.

In the HT phase, the unit cell contains only one molecule (Z' = 0.5) having largely disordered terminal ethyl moieties (Fig. 3). The two asymmetrical molecular units in the RT phase converged to one asymmetrical unit, probably due to the effect of thermal motion. The centroids of the molecules in the HT phase were aligned along the *a*-axis. The distance between the π-conjugated system of DE2 was 3.812 Å, whereas in the RT phase there are two different packing distances, one is a

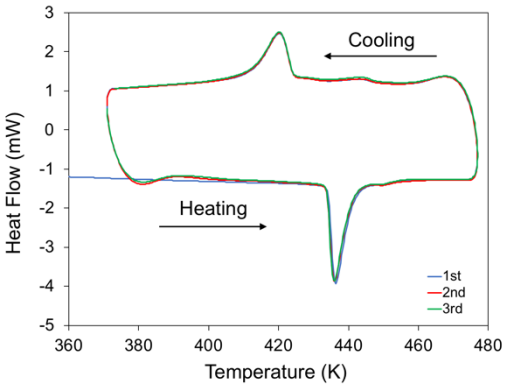

Fig. 1 DSC curve of the DE2 crystal at a 20 K min^{-1} heating/cooling rate in a heating-cooling cycle.

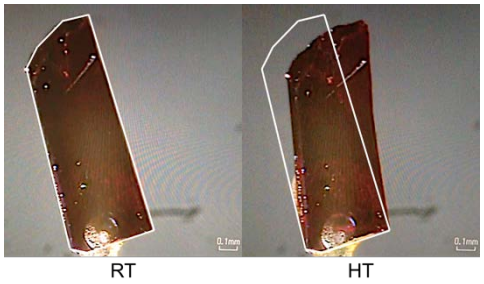

Fig. 2 Shape changes of a single crystal of DE2 during its phase transition (RT phase: left, HT phase: right).

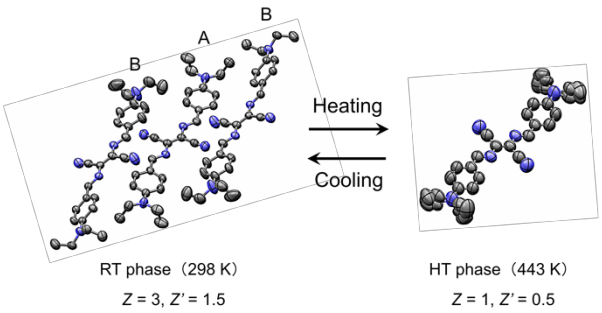

Fig. 3 Molecular conformations of DE2 in RT and HT phases.

distance between molecules A and B (4.531 Å), and the other is between the B molecules (3.847 Å). The superposition of the packing diagram of both phases clearly indicated that there is no significant difference in the molecular arrangement between the two phases, although the positions of the molecular centroids were slightly displaced (Fig. S4, ESI †). The length of the *a*-axis in the HT phase (7.235 Å) is comparable to the length of the centroids of the two neighboring B molecules in the RT phase (7.190 Å). The *b*-axis in the HT phase corresponds to the *a*-axis in the RT phase. The *c*-axis in the HT phase corresponds to the length between the molecular centroids placed approximately along the [0 -1 1] direction in the RT phase.

A considerable lattice contraction was observed along the stacking direction. The centroid distance for four A-B-B-A molecules in the RT phase was 23.089 Å and the corresponding centroid distance for the four molecules in the HT phase was 21.705 Å, which is estimated to decrease by approximately 5.99% (Fig. S5a, ESI †). Conversely, the centroid distance along the short molecular axis increased in the HT phase. The corresponding distance in the RT phase is 9.225 Å (*a*-axis), whereas that in the HT phase is 9.519 Å (*b*-axis), which increased by approximately 3.19% after phase transition (Fig. S5b, ESI †). Fig. 4 shows crystal faces with the corresponding molecular arrangement for both phases. The long crystal growth direction of the DE2 crystals corresponded to the stacking direction in both phases. The direction along the short molecular axis is parallel to the thickness direction of the crystal. Photographic

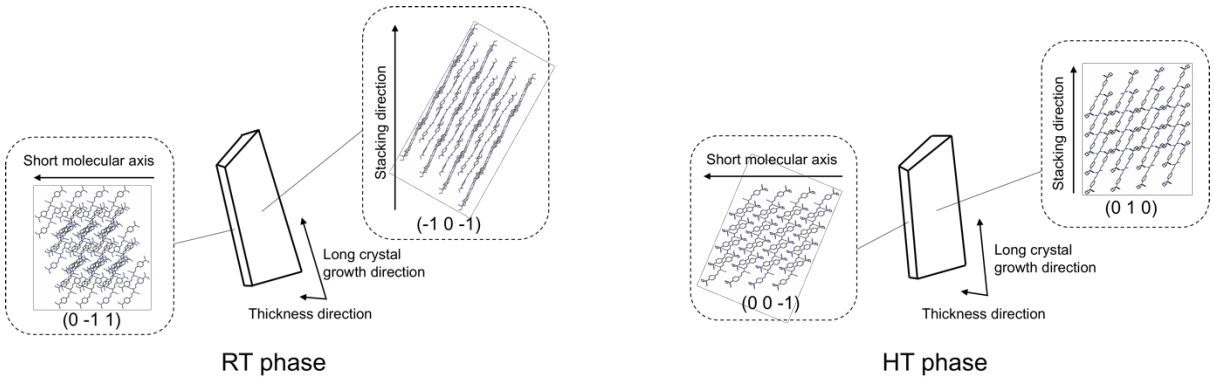

Fig. 4 Face indices of single crystals of DE2 in RT and HT phases.

analysis of the dynamic motion of the DE2 crystal showed that the length of the long crystal growth direction decreased from 1.157 mm to 1.086 mm and the length of the thickness direction increased from 0.151 mm to 0.155 mm. The rate for the size change in both directions from the RT to HT is -6.14% and +2.65%, respectively. This is consistent with the distance change observed from X-ray structural analysis.

To investigate the detailed structural changes of the DE2 crystal upon heating from the RT to HT phase, temperature-dependent structure analysis was performed at every 50 K interval from 143 to 393 K. The results showed that the structures from 143 to 393 K adopted the RT phase (Table S2). From 143 to 393 K, an anisotropic change in the unit cell parameters was observed. The increase in the *b*-axis was larger than that in the *a*- and *c*-axes (Table S3).

Four geometric parameters were evaluated to measure the temperature-dependent change of molecular arrangement: distances between the molecular centroids of A-B and that of B-B along the stacking direction, and between the centroids of a neighboring molecular pair on the same molecular plane along the long and short molecular axes directions (Fig. 5 and Fig. S6, ESI †). These parameters gradually increased upon heating

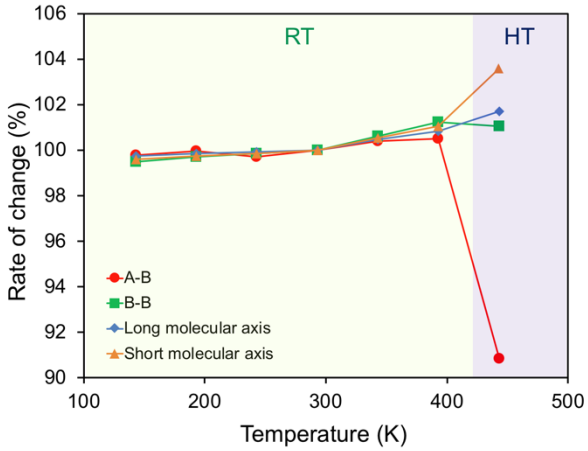

Fig. 5 Temperature dependence of the four selected distances between the molecular centroids. (The vertical axis indicates the rate of change of each centroid distance at a specific temperature with respect to the centroid distance at 293 K.)

from 143 to 393 K. Furthermore, the distance between the molecular centroids of B-B along the stacking direction increased by 1.74%, larger than the others in the RT phase. The changes of these parameters could also be macroscopically observed by microscopic measurement of the crystal upon heating and cooling (movie S7, ESI †). The crystal expanded upon heating before the phase transition and contracted upon cooling after the transition to the RT phase. Fig. 5 also shows the anisotropic changes of the distances of the molecular centroids during the phase transition. Upon phase transition, the distances between the molecular centroids of A-B and of B-B along the stacking direction decreased, although the distances between the molecular centroids along the long and short molecular axes increased. The macroscopic shape change of the crystal resulting from the increase in the long molecular axis direction was difficult to observe because the rate of change was small (0.86%) and the direction was not parallel to either the long crystal growth direction or thickness direction.

Changes in isotropic temperature factors (U_{iso}) of the carbon atoms of the terminal ethyl groups in the RT phase (Fig. S7, ESI †) suggest that the thermal motion of the terminal substituents greatly influences the relatively large change in the distance along the stacking direction.[35] Further measurements are required to understand the structure-property relationship with respect to this interesting motion of the crystals. Derivatives of DE2 with different terminal alkyl groups will also be studied in terms of the effect of alkyl chain length on this behavior in the future.

In summary, we reported the first example of a metal-free organic dye that exhibits macroscopic crystalline deformation caused by an alkyl disorder. The DE2 crystal shape observably changed by approximately 6% along the long crystal growth direction and the change was reversible. X-ray structural analysis revealed that the distances of the molecular centroids anisotropically changed during the phase transition. Macroscopic crystalline deformation occurred due to the slight rearrangement of the molecules, which is presumably correlated with the disorder of ethyl moieties in the high-temperature region.

Conflicts of interest

There are no conflicts of interest to declare.

Notes and references

1 H. Jiang, S. Kelch, A. Lendlein, *Adv. Mater.,* 2006, **18**, 1471.
2 T. Ikeda, J. Mamiya, Y. Yu, *Angew. Chem. Int. Ed.*, 2007, **46**, 506.
3 H. J. Shepherd, I. A. Gural'skiy, C. M. Quintero, S. Tricard, L. Salmon, G. Moln μ r, A. Bousseksou, *Nat. Commun.*, 2013, **4**, 2607.
4 A. Lendlein, H. Jiang, O. Ju¨nger, R. Langer, *Nature*, 2005, **434**, 879.
5 D. H. Wang, K. M. Lee, Z. Yu, H. Koerner, R. A. Vaia, T. J. White, L.-S. Tan, *Macromolecules,* 2011, **44**, 3840.
6 K. M. Lee, T. J. White, *Macromolecules*, 2012, **45**, 7163.
7 W. Wu, L. Yao, T. Yang, R. Yin, F. Li, Y. Yu, *J. Am. Chem. Soc.*, 2011, **133**, 15810.
8 K. Iwaso, Y. Takashima, A. Harada, *Nat. Chem.*, 2016, **8**, 625.
9 H. Koshima, N. Ojima, H. Uchimoto, *J. Am. Chem. Soc.*, 2009, **131**, 96891.
10 G. Liu, J. Liu, X. Ye, L. Nie, P. Gu, X. Tao, Q. Zhang, *Angew. Chem. Int. Ed.*, 2017, **56**, 198.
11 S. Kobatake, S. Takami, H. Muto, T. Ishikawa, M. Irie, *Nature*, 2007, **446**, 778.
12 D. Das, T. Jacobs, L. J. Barbour, *Nat. Mater.*, 2010, **9**, 36.
13 Y.-G. Huang, Y. Shiota, S.-Q. Su, S.-Q. Wu, Z.-S. Yao, G.-L. Li, S. Kanegawa, S. Kang, T. Kamachi, K. Yoshizawa, K. Ariga, O. Sato, *Angew. Chem. Int. Ed.*, 2016, **55**, 14628.
14 P. Commins, I. T. Desta, D. P. Karothu, M. K. Panda P. Naumov, *Chem. Commun.*, 2016, **52**, 13941.
15 P. Naumov, S. Chizhik, M. K. Panda, N. K. Nath, E. Boldyreva, *Chem. Rev.*, 2015, **115**, 12440.
16 M. C. Etter, A. R. Siedle, *J. Am. Chem. Soc.*, 1983, **105**, 641.
17 S. C. Sahoo, M. K. Panda, N. K. Nath, P. Naumov, *J. Am. Chem. Soc.*, 2013, **135**, 12241.
18 S. C. Sahoo, S. B. Sinha, M. S. R. N. Kiran, U. Ramamurty, A. F. Dericioglu, C. M. Reddy, P. Naumov, *J. Am. Chem. Soc.*, 2013, **135**, 13843.
19 M. K. Panda, T. Runcěvski, A. Husain, R. E. Dinnebier, P. Naumov, *J. Am. Chem. Soc.*, 2015, **137**, 1895.
20 M. K. Panda, T. Runcˇevski, S. C. Sahoo, A. A. Belik, N. K. Nath, R. E. Dinnebier, P. Naumov, *Nat. Commun.*, 2014, **5**, 4811.
21 N. K. Nath, M. K. Panda, S. C. Sahoo, P. Naumov, *CrystEngComm*, 2014, **16**, 1850.
22 M. K. Panda, R. Centore, M. Causà, A. Tuzi, F. Borbone, P. Naumov, *Sci. Rep.*, 2016, **6**, 29610.
23 S.-Q. Su, T. Kamachi, Z.-S. Yao, Y.-G. Huang, Y. Shiota, K. Yoshizawa, N. Azuma, Y. Miyazaki, M. Nakano, G. Maruta, S. Takeda, S. Kang, S. Kanegawa, O. Sato, *Nat. Commun.*, 2015, **6**, 9810.
24 Z.-S. Yao, M. Mito, T. Kamachi, Y. Shiota, K. Yoshizawa, N. Azuma, Y. Miyazaki, K. Takahashi, K. Zhang, T. Nakanishi, S. Kang, S. Kanegawa, O. Sato, *Nat. Chem.*, 2014, **6**, 1079.
25 K. Shirai, M. Matsuoka, K. Fukunishi, *Dyes Pigm.*, 2000, **47**, 107.
26 S. Matsumoto, T. Kobayashi, T. Aoyama, T. Wada, *Chem. Commun.*, 2003, 1910.
27 T. Kobayashi, S. Matsumoto, T. Tanaka, H. Kunugita, K. Ema, T. Aoyama, T. Wada, *Phys. Chem. Chem. Phys.*, 2005, **7**, 1726.
28 K. Kinashi, K.-P. Lee, S. Matsumoto, K. Ishida, Y. Ueda, *Dyes Pigm.*, 2011, **92**, 783.
29 T. Hosokai, T. Aoyama, T. Kobayashi, A. Nakao, S. Matsumoto, *Chem. Phys. Lett.*, 2010, **487**, 77.
30 T. Tanaka, S. Matsumoto, T. Kobayashi, M. Satoh, T. Aoyama, *J. Phys. Chem. C*, 2011, **115**, 19598.
31 J.C. Ribierre, M. Sato, A. Ishizuka, T. Tanaka, S. Watanabe, M. Matsumoto, S. Matsumoto, M. Uchiyama, T. Aoyama, *Org. Electron.*, 2012, **13**, 999.
32 J. C. Ribierre, Y. Yokota, M. Satoh, A. Ishizuka, T. Tanaka, S. Watanabe, M. Matsumoto, A. Muranaka, S. Matsumoto, M. Uchiyama, T. Aoyama, *RSC Adv.*, 2014, **4**, 36729.
33 S. Matsumoto, K. Shirai, K. Kobayashi, T. Wada, M. Shiro, *Z. Kristallogr.*, 2004, **219**, 239.
34 T. Jindo, B.-S. Kim, Y. Akune, E. Horiguchi-Babamoto, K.-P. Lee, K. Kinashi, Y. Ueda, S. Matsumoto, *Z. Kristallogr.*, 2016, **231**, 487.
35 T. Shima, T. Muraoka, N. Hoshino, T. Akutagawa, Y. Kobayashi, K. Kinbara, *Angew. Chem. Int. Ed.*, 2014, **53**, 7173.